THE JOURNAL OF BIOLOGICAL CHEMISTRY
Vol. 276, No. 25, Issue of June 22, pp. 23056–23064, 2001

Printed in U.S.A.

A Spirochete Surface Protein Uncouples Store-operated Calcium Channels in Fibroblasts

A NOVEL CYTOTOXIC MECHANISM*

Received for publication, December 27, 2000, and in revised form, April 11, 2001
Published, JBC Papers in Press, April 18, 2001, DOI 10.1074/jbc.M011735200

Qin Wang‡, Kevin S. Ko§¶, András Kapus‖, Christopher A. G. McCulloch§, and Richard P. Ellen‡**

From the ‡Dental Research Institute, the §Canadian Institutes of Health Research Group in Periodontal Physiology, Faculty of Dentistry, and the ‖Department of Surgery, University of Toronto and the Division of Surgery, Toronto General Hospital, Toronto, Ontario M5G 1G6, Canada

The cytotoxicity of infectious agents can be mediated by disruption of calcium signaling in target cells. Outer membrane proteins of the spirochete *Treponema denticola*, a periodontal pathogen, inhibit agonist-induced Ca^{2+} release from internal stores in gingival fibroblasts, but the mechanism is not defined. We determined here that the major surface protein (Msp) of *T. denticola* perturbs calcium signaling in human fibroblasts by uncoupling store-operated channels. Msp localized in complexes on the cell surface. Ratio fluorimetry showed that in cells loaded with fura-2 or fura-C18, Msp induced cytoplasmic and near-plasma membrane Ca^{2+} transients, respectively. Increased conductance was confirmed by fluorescence quenching of fura-2-loaded cells with Mn^{2+} after Msp treatment. Calcium entry was blocked with anti-Msp antibodies and inhibited by chelating external Ca^{2+} with EGTA. Msp pretreatment reduced the amplitude of $[Ca^{2+}]_i$ transients upon challenge with ATP or thapsigargin. In experiments using cells loaded with mag-fura-2 to report endoplasmic reticulum Ca^{2+}, Msp reduced Ca^{2+} efflux from endoplasmic reticulum stores when ATP was used as an agonist. Msp alone did not induce Ca^{2+} release from these stores. Msp inhibited store-operated influx of extracellular calcium following intracellular Ca^{2+} depletion by thapsigargin and also promoted the assembly of subcortical actin filaments. This actin assembly was blocked by chelating intracellular Ca^{2+} with 1,2-bis(2-aminophenoxy)ethane-*N*,*N*,*N*′,*N*′-tetraacetic acid acetoxymethyl ester. The reduced amplitude of agonist-induced transients and inhibition of store-operated Ca^{2+} entry due to Msp were reversed by latrunculin B, an inhibitor of actin filament assembly. Thus, Msp retards Ca^{2+} release from endoplasmic reticulum stores, and it inhibits subsequent Ca^{2+} influx by uncoupling store-operated channels. Actin filament rearrangement coincident with conformational uncoupling of store-operated calcium fluxes is a novel mechanism by which surface proteins and toxins of pathogenic microorganisms may damage host cells.

What if pathogenic microorganisms were able to disrupt the regulation of intracellular calcium signals in host cells? They would disturb a critical signaling pathway by which eukaryotic cells respond to external stimuli (1) and would impair crucial downstream functions by which cells maintain homeostasis. For example, calcium ion concentration ($[Ca^{2+}]_i$)[1] regulates the assembly and turnover of actin filaments (2), which in turn controls cell shape, volume regulation, locomotion, and phagocytosis. These are essential functions for maintaining tissue integrity, for promoting wound healing, and for mediating protection from infection.

Many human cells regulate calcium homeostasis using store-operated calcium fluxes, a system in which Ca^{2+} influx through store-operated channels (SOCs) in the plasma membrane is stimulated by the depletion of Ca^{2+} in internal stores in the lumen of the endoplasmic reticulum (ER) (3, 4). A variety of potential cytotoxins of insects, reptiles, and microorganisms affect ion channel function (5–7). These toxins may include the surface molecules of opportunistic or overtly pathogenic bacteria, including some that cause cytoskeletal perturbation or that form ion channels in the host cell plasma membrane. Several microbial products have been reported to alter ion transport, but none is known to uncouple Ca^{2+} ER stores and SOCs.

Although the mechanisms by which transient Ca^{2+} depletion in the ER triggers Ca^{2+} influx through SOCs are not well understood, one compelling model is based on the physical proximity between the plasma membrane and the ER (1). This system may involve the inositol trisphosphate receptor on the ER as a mediator of the functional coupling of ER store depletion and Ca^{2+} entry through the plasma membrane (8, 9). Notably, the assembly and disassembly of actin filaments subjacent to the plasma membrane is a major determinant of reversible coupling of the ER and plasma membrane and thereby modulates the signals that regulate Ca^{2+} influx through SOCs (8, 10).

Whole cells and outer membrane proteins of the oral spirochete *Treponema denticola* exert profound effects on actin assembly in cultured human gingival fibroblasts and epithelial cells (11–14). These properties may contribute to bacterial pathogenicity by impeding actin-dependent functions that are crucial for homeostasis of gingival tissues (15, 16). Since actin assembly is highly sensitive to fluctuations in calcium concentration (2), it is notable that outer membrane fractions of *T.*

* This work was supported by Canadian Institutes of Health Research (CIHR) Grant MOP-5619, a maintenance grant, and a group grant. The costs of publication of this article were defrayed in part by the payment of page charges. This article must therefore be hereby marked "*advertisement*" in accordance with 18 U.S.C. Section 1734 solely to indicate this fact.

The nucleotide sequence(s) reported in this paper has been submitted to the GenBank™/EBI Data Bank with accession number(s) U66256.

¶ Supported by a CIHR fellowship.

** To whom correspondence should be addressed. Tel.: 416-979-4917 (ext. 1–4456); Fax: 416-979-4936; E-mail: richard.ellen@utoronto.ca.

[1] The abbreviations used are: $[Ca^{2+}]_i$ and $[Ca^{2+}]_{ER}$, intracellular and ER calcium ion concentration, respectively; ER, endoplasmic reticulum; SOC, store-operated channel; Msp, major surface protein; 2-APB, 2-aminoethoxydiphenyl borate.

denticola inhibit inositol phosphate and intracellular calcium responses of fibroblasts to chemical agonists (14, 17). Since cortical actin and the inositol trisphosphate receptor are evidently important in the regulation of store-operated calcium channels in a variety of cell types (8, 18–20), we hypothesized that the major surface protein of *T. denticola*, Msp,[2] may be one of the outer membrane proteins that is responsible for bacterial perturbation of calcium flux in cells from the periodontium. We examined the effects of Msp on calcium homeostasis in gingival fibroblasts and report that Msp mediates calcium transients and inhibits SOC activation by promoting assembly of subcortical actin filaments. These filaments in turn uncouple the ER from SOCs. Our results provide a novel mechanism by which pathogenic bacteria may subvert host cell signaling systems and thereby contribute to loss of tissue homeostasis in chronic infections such as periodontitis.

EXPERIMENTAL PROCEDURES

Reagents—Bovine serum albumin, Texas Red-conjugated goat anti-rabbit antibodies, thapsigargin, ATP, ionomycin, latrunculin B, and valinomycin were purchased from Sigma. Fura-2/AM, mag-fura-2/AM, fura-C18, 1,2-bis(2-aminophenoxy)ethane-*N*,*N*,*N*′,*N*′-tetraacetic acid acetoxymethyl ester, bis-[1,3-dibutylbarbituric acid]trimethineoxonol, and rhodamine phalloidin were obtained from Molecular Probes, Inc. (Eugene, OR). 2-Aminoethoxydiphenyl borate (2-APB) was obtained from Calbiochem.

Preparation of Msp—Msp is an immunogenic surface protein of *T. denticola* that complexes with a serine protease, PrtP, in the outer sheath of the bacterium. Msp was prepared from *T. denticola* type strain ATCC 35405, as previously described (21, 22), with the following modifications. The starting material was ~8 g, wet weight, per 4-liter bacterial culture in late logarithmic growth phase. After the deoxycholate and the *n*-octylpolyoxyethylene extraction steps and ultracentrifugation, the enriched Msp solution was incubated for 7 days at 37 °C until peptidase activity could no longer be detected by the chromogenic peptides *N*-succinyl-L-alanyl-L-alanyl-L-prolyl-L-phenylalanine nitroanilide and N-benzoyl-DL-arginine-*p*-nitroanilide (Sigma) (23). The enriched protein solution was concentrated ~30-fold by Amicon ultrafiltration (Amicon Concentricon plus 80, Amicon Inc., Beverly, MA). After washing with 5 liters of 10 mM Tris (pH 8.0), five washings with double-distilled water, and ultracentrifugation for 2 h to remove trace amounts of detergent, the Msp was dissolved and dialyzed against double-distilled water. The protein content was determined by Bio-Rad assay using bovine serum albumin as a standard.

For all experiments (except dose-response experiments), a 1:100 dilution of Msp in calcium buffer was used. This preparation contained 0.41 mg of protein (dry weight) per ml. A final concentration of 30 μg of protein/ml, corresponding to ~160 nM, was used for most challenge assays of cells. When pretreatment with Msp was specified, the Msp remained in the cell culture wells for the duration of the experiment unless mentioned. In some experiments, Msp was boiled for 10 min to denature proteins or heated at 60 °C for 30 min. In other experiments, the cells were pretreated with a mixture of Msp and anti-Msp antibodies at a 2:3 ratio (protein concentration) that had been preincubated for 60 min.

Gel Electrophoresis and Immunoblotting—SDS-polyacrylamide gel electrophoresis was performed as previously described in 10% (w/v) polyacrylamide gels with a current of 200 V (24, 25). Proteins or peptides were solubilized in sample buffer either at room temperature or heated at 100 °C for 5 min prior to electrophoresis and staining with Coomassie Brilliant Blue. For immunoblotting, proteins were transferred electrophoretically to nitrocellulose membranes (26). Following transfer, membranes were blocked with 5% bovine serum albumin in Tris-buffered saline (20 mM Tris, 0.5 M NaCl, pH 7.6) and probed with rabbit polyclonal antibodies raised against Msp of ATCC 35405, kindly provided by B. C. McBride and P. Hannam (27). After incubation with horseradish peroxidase-conjugated secondary antibodies at appropriate dilutions, enhanced chemiluminescence (Amersham Pharmacia Biotech) was used to detect the signal.

Cell Culture—Human gingival fibroblasts were derived from primary explant cultures as described (28). Cells from passages 6–15 were grown as monolayers in T-75 flasks in α-minimal essential medium with 10% fetal bovine serum and antibiotics. Cells from these cultures were harvested and replated onto glass coverslips 2 days before each experiment, as described previously (17). The cells were grown to confluence prior to all experiments except when sparse cultures were used as indicated.

Intracellular Calcium—For measurement of whole cell intracellular calcium ion concentration ($[Ca^{2+}]_i$), cells on coverslips were loaded with 3 μM fura-2/AM (a Ca^{2+}-sensitive fluorescent dye) for 20 min at 37 °C (17). For measurement of near-plasma membrane Ca^{2+} concentration, cells attached to coverslips were briefly permeabilized with saponin and incubated with 2 μM fura-C18, pentapotassium salt (29) at 25 °C for 10 min followed by three washes with PBS. For estimation of $[Ca^{2+}]_{ER}$, cells on coverslips were incubated with mag-fura-2/AM (4 μM) (30) for 150 min at 37 °C, in α-minimal essential medium containing fetal bovine serum (10%) (31). The calcium-free buffer consisted of a bicarbonate-free medium containing 150 mM NaCl, 5 mM KCl, 10 mM D-glucose, 1 mM $MgSO_4$, 1 mM Na_2HPO_4, and 20 mM HEPES at pH 7.4 with an osmolarity of 291 mosM. For experiments requiring external calcium, 1 mM $CaC1_2$ was added to the buffer; for experiments requiring chelation of external Ca^{2+}, 2 mM EGTA was added. F_{max} and F_{min} were determined using ionomycin and EGTA as described previously (17).

After incubation with fura-2/AM, inspection of cells by fluorescence microscopy demonstrated no vesicular compartmentalization of fura-2, suggesting that the dye loading method permitted measurement of cytosolic $[Ca^{2+}]_i$. Visual inspection of fura-C18-loaded cells and mag-fura-2-loaded cells showed fluorescent labeling of the plasma membrane and intracellular organelles, respectively. Estimates of whole cell $[Ca^{2+}]_i$ and near plasma membrane $[Ca^{2+}]_i$ were calculated according to the equation of Grynkiewicz (32) from the emitted fluorescence measurements, using a Nikon Diaphot II inverted microscope optically interfaced to a Deltascan 4000, dual beam, epifluorescence spectrofluorimeter and analysis system (Photon Technology Int., London, Ontario, Canada), as described previously (17).

Msp Perturbation of Calcium Fluxes—To examine the effect of Msp on internal release of Ca^{2+}, ATP (100 μM; Sigma) and thapsigargin (1 μM; Sigma) were used as agonists and added to resting cells in calcium-free buffer with EGTA (17). Cells that were pretreated with Msp for 40 min at 25 °C were compared with untreated cells. To compare the function of SOCs in these cells, the influx of extracellular calcium following depletion of intracellular stores was also studied. Fibroblasts were exposed to 1 μM thapsigargin in 1 mM EGTA buffer for 30 min to deplete internal Ca^{2+} and to chelate residual extracellular Ca^{2+}. $CaCl_2$ (2 mM) was added, and $[Ca^{2+}]_i$ increases due to calcium influx were measured. These experiments were repeated in cells pretreated with 1 μM latrunculin B (30 min, 25 °C), an inhibitor of actin polymerization.

In some experiments, the influx pathway was examined after the addition of Msp or water vehicle in cells loaded with fura-2. We measured the fluorescence of single cells at the isosbestic point (356 nm) in the presence of $MnCl_2$ (1 mM) in the standard Ca^{2+}-containing buffer (33). For indirect assessment of general cation permeability of the plasma membrane to monovalent cations, we measured membrane potential using flow cytometry and the bisoxonol dye bis-[1,3-dibutylbarbituric acid]trimethineoxonol (3) as described (34).

Immunocytochemistry and Confocal Microscopy—To examine the location of Msp binding to cells, indirect immunofluorescence microscopy was performed on Msp-pretreated cells using polyclonal anti-Msp-antibodies as the primary antibody. Cells grown on coverslips were fixed and permeabilized with methanol at −20 °C for 10 min, blocked with 1:1000 mouse serum in PBS for 10 min, incubated with primary antibody (1:100 dilution) for 1 h at room temperature, washed three times with PBS containing 0.2% bovine serum albumin, and incubated with Texas Red-conjugated goat-anti-rabbit antibodies (1:100). The coverslips were washed with PBS and mounted with an antifade mounting medium (ICN, Montreal, Canada). The fibroblasts were examined using a × 40, 1.3 NA oil immersion objective under epifluorescence optics (Leica CLSM, Heidelberg, Germany).

Laser-scanning confocal microscopy (Leica CLSM) was used to examine actin filament assembly induced by Msp. The cells were fixed in 3% paraformaldehyde for 15 min, permeabilized in 0.2% Triton X-100 for 5 min, and stained with rhodamine phalloidin (35). The excitation filter used was 530/20 nm, and emitted fluorescence was collected through an emission filter (620/40 nm). Cells were imaged with a × 63 oil immersion lens, 1.4 NA, and transverse optical sections were obtained in 1-μm steps from the level of cell attachment at the substratum to the dorsal surface of the cell (33). In some experiments, the fluorescence intensity of rhodamine phalloidin staining was measured with a fluorescence spectrophotometer (Leitz MVP; Wetzlar, Germany) (28) in

[2] The amino acid sequence of Msp protein can be accessed through NCBI protein data base under NCBI accession number AAB47939 (51).

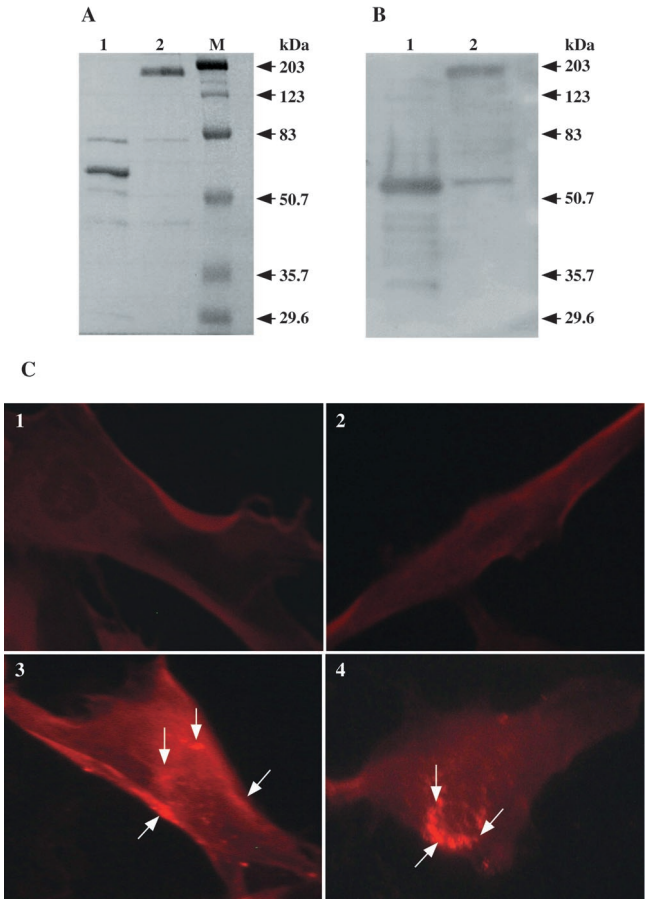

FIG. 1. **Enriched Msp complex and immunolocalization of Msp on fibroblasts.** *A*, Msp was prepared as described in "Experimental Procedures" and Refs. 21 and 22, subjected to SDS-polyacrylamide gel electrophoresis, and stained with Coomassie Brilliant Blue. *Lane 1*, boiled preparation; *lane 2*, unheated Msp preparation; *lane M*, molecular mass standards. *B*, immunoblot. *Lane 1*, boiled preparation; *lane 2*, unheated Msp preparation. *C*, indirect immunofluorescence microscopy of cells incubated with Msp (30 μg/ml, 25 °C, 30 min). *1*, secondary antibody control labeled only with Texas Red-conjugated goat anti-rabbit antibody shows a small amount of nonspecific staining and autofluorescence. *2*, similar results were obtained with primary anti-Msp control but with no secondary goat anti-rabbit conjugate. Cells incubated with Msp for 1 min (*3*) or 30 min (*4*) and stained with both primary anti-Msp and secondary goat anti-rabbit conjugate show specific fluorescence staining along cell membranes. Note the clustering of Msp to one pole of cell at 30 min postincubation with Msp.

square sampling zones (25 μm^2) immediately beneath the cell membrane.

Cell Viability—Propidium iodide staining was used to determine if Msp was toxic to cells during the duration of the experiments. Flow cytometry analyses were performed as described (36). Briefly, cells were trypsinized and suspended in PBS, pelleted, resuspended in PBS to a cell concentration of 1×10^6/ml, and stained with propidium iodide (10 μl/ml; Calbiochem). After a 5-min incubation, cells were analyzed by flow cytometry.

Data Analysis—Means and S.E. values were calculated for $[Ca^{2+}]_i$ measurements. Calcium measurements were restricted to (i) base-line $[Ca^{2+}]_i$; (ii) percentage change of the transient $[Ca^{2+}]_i$ above base-line; (iii) net change in $[Ca^{2+}]_i$ above base line; and (iv) time to peak $[Ca^{2+}]_i$. For continuous variable data, means and S.E. of $[Ca^{2+}]_i$ were computed, and, when appropriate, comparisons between two groups were made with the unpaired Student's *t* test with statistical significance set at $p < 0.05$.

RESULTS

Preparation of Msp—The Msp preparation was highly enriched by sequential detergent extraction and autoproteolysis of *T. denticola* extracts. We isolated a fraction that contained primarily Msp oligomers, which migrated as a single ~190-kDa band in SDS-polyacrylamide gel electrophoresis (21) (Fig. 1*A*). Boiled samples demonstrated a 53-kDa polypeptide that is known to be the monomer (27, 37). The 95-kDa chymotrypsin-like protease that usually associates with Msp in the outer membrane was not detected in the gels; nor was its peptidase activity detected. Immunoblots of the preparation using anti-Msp antibodies showed almost exclusive staining of the prominent 190-kDa oligomer and the 53-kDa monomer in native and heat-denatured preparations, respectively (Fig. 1*B*), confirming that these bands contained the authentic Msp from *T. denticola*.

Previous studies demonstrated that Msp binds to fibronectin, fibrinogen, and laminin and associates with epithelial cell surfaces and cytoplasmic membrane proteins (22, 37). When the Msp preparation was incubated with fibroblasts, immunostaining showed that Msp associated with the fibroblast surface (Fig. 1*C*). After a 30-min incubation, intense Msp staining was clustered in one area of the cell, indicating a capping phenomenon and possible aggregation of ligand-bound receptors.

Msp Induces Ca^{2+} Transients—Single cell ratio fluorimetry was used to test whether the association of Msp with the fibroblast plasma membrane caused perturbation of calcium homeostasis. For all experiments, $[Ca^{2+}]_i$ was stable in untreated cells, even over prolonged time course experiments (>120 min). In calcium buffer, exposure of cells to Msp induced a robust Ca^{2+} transient that often returned to a level ~15–30% higher than base-line within 90 s of the peak (Fig. 2, *A–C*); subsequent smaller transients could also be detected over a period of 30 min in some cells (Fig. 2*B*, *inset*). Treatment of cells with increasing concentrations of Msp (1, 10, 30 μg/ml) showed a dose-response relationship with the amplitude of the calcium peak (Fig. 2*H*). In control cells treated with the vehicle (distilled H_2O added to cell culture buffer), there was no Ca^{2+} response (Fig. 2*D*), indicating that the Msp-induced Ca^{2+} responses were not simply due to physical disturbance or an anisosmotic change. Further, only cells with bright fura-2 staining in the cytoplasm were included in analyses to overcome the possibility of measuring dead or dying cells (see data on cell death below). In cells challenged with Msp that was preincubated with anti-Msp antibodies, there was no Ca^{2+} response detected upon the addition of Msp (Fig. 2*E*), indicating that the Msp-induced transient was due to a specific interaction between Msp and the cells. Boiling the Msp eliminated the Ca^{2+} response (Fig. 2*F*); the amplitude of the Ca^{2+} transient was much lower than controls when the Msp was heated to 60 °C for 30 min (Fig. 2*G*). Thus, the ability of Msp to interact with cells and to generate Ca^{2+} responses evidently depends on the undenatured protein complex. Finally, cells that were incubated repeatedly with fresh doses of Msp showed progressively diminished calcium responses (Fig. 2*I*).

To determine if Msp could induce Ca^{2+} transients subjacent to the cell membrane, cells were loaded with fura-C18. In these experiments Msp evoked large amplitude calcium transients, demonstrating a sharp elevation of $[Ca^{2+}]_i$ near the plasma membrane (Fig. 2*J*). These transients occurred more rapidly than the cytoplasmic calcium signals following Msp treatment ($n = 10$ experiments; $p < 0.05$), indicating that Msp may stimulate Ca^{2+} influx through plasma membrane-permeable channels. We determined the source of Ca^{2+} for the observed rise in $[Ca^{2+}]_i$. Fura-2-loaded cells were incubated in Ca^{2+}-free buffer containing EGTA. The cells were rapidly switched to the EGTA buffer prior to the addition of Msp to avoid depletion of intracellular stores. Under these conditions, Msp treatment failed to evoke a defined Ca^{2+} transient (Fig. 2*K*), indicating that most of the Ca^{2+} for the robust intracellular response was probably derived from influx through plasma membrane-per-

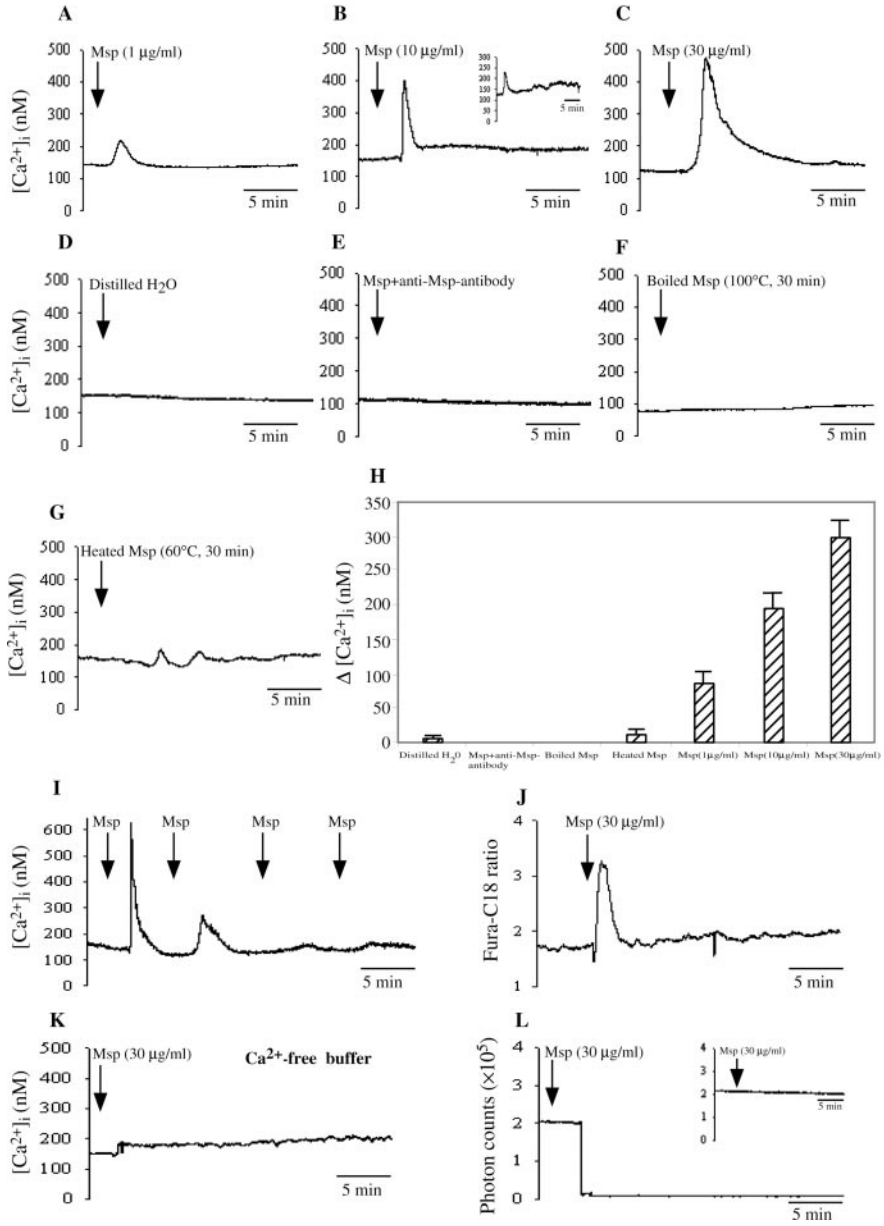

FIG. 2. **Msp induces Ca^{2+} transients in fibroblasts.** *A–C*, cells were treated with Msp as indicated (1 μg/ml, 10 μg/l, 30 μg/ml) in 1 mM Ca^{2+} buffer, and intracellular calcium ($[Ca^{2+}]_i$) was measured in fura-2-loaded cells by ratio fluorimetry. There was a ~90-s delay after incubation, presumably due to Msp binding to cell surface fibronectin. *B* (*inset*), an example of prolonged post-transient fluctuations of $[Ca^{2+}]_i$ observed in many cells treated with Msp at 10 and 30 μg/ml. *D*, cells were treated with distilled H_2O added to cell culture medium. *E*, cells were treated with Msp after incubation with anti-Msp antibody (2:3 protein ratio). *F*, cells were treated with boiled Msp (30 μg/ml, 100 °C, 30 min). *G*, cells were treated with heated Msp (30 μg/ml, 60 °C, 30 min). *H*, summary of increases of $[Ca^{2+}]_i$ above unstimulated control values (data from n = 9 experiments; means ± S.E.; values in nM). Data show increased $[Ca^{2+}]_i$ above base-line after the addition of distilled H_2O to cell culture medium, Msp following anti-Msp antibody, boiled Msp, heated Msp, or Msp at the indicated concentrations. All experiments were performed in calcium buffer (1 mM). *I*, cells incubated repeatedly with fresh doses of Msp (30 μg/ml) but without wash-out showed no response. *J*, cells loaded with the membrane-linked calcium reporter dye fura-C18 and treated with Msp (30 μg/ml) produced large amplitude rise of submembrane $[Ca^{2+}]_i$. A similar result was obtained in n = 5 cells. *K*, Msp failed to evoke Ca^{2+} transients in cells incubated in calcium-free buffer augmented with EGTA (2 mM); similar results were seen in n = 8 cells. *L*, typical traces of photon counts of single cells showing a sharp decline in the fluorescence of fura-2 excited at 356 nm ~2 min after the addition of Msp in buffer containing manganese chloride (1 mM). The loss of fluorescence after the addition of Msp was contemporaneous with Msp-induced calcium transients (~90 s; see Fig. 1*C*). The data are representative of five independent experiments. The *inset* in *L* shows Msp-treated cells in medium without manganese chloride.

meable channels. We examined the influx pathway further by performing quenching experiments in which the extracellular bathing buffer was supplemented with 1 mM $MnCl_2$ and the fluorescence of fura-2 was excited at 356 nm (the isosbestic or calcium-insensitive point) (33). When single emission photon counts were measured, cells demonstrated a drop in fluorescence ~90 s after Msp was added to the culture medium, probably due to influx of Mn^{2+} and fluorescence quenching of fura-2 (Fig. 2*L*). These results indicate that the Msp-induced Ca^{2+} transient is due to entry from the extracellular medium.

To assess whether Msp causes a general increase in cation permeability, we measured the membrane potential with the bisoxonol dye bis-[1,3-dibutylbarbituric acid]trimethineoxonol and flow cytometry. Measurement of bis-[1,3-dibutylbarbituric acid]trimethineoxonol fluorescence after vehicle or Msp treatment showed only a 2% reduction of fluorescence, while KCl depolarization in the presence of valinomycin (3 μM) produced large reductions (~25% reductions after each of the sequential additions of 50 mM KCl; 5000 cells/run). Experiments conducted with calcium buffer and ionomycin (2 μM) treatments indicated that cells preincubated with Msp or vehicle responded with an equivalent increase in $[Ca^{2+}]_i$ ($p > 0.2$; n = 5 cells each). These data indicated that the cell membranes of Msp-treated cells were intact. Consistent with these observations, the basal $[Ca^{2+}]_i$ was unchanged in Msp-treated and vehicle-treated cells (~150 nM).

We determined if Msp is cytotoxic to fibroblasts in the short term (*i.e.* under the conditions used for these experiments) because of a rise in intracellular Ca^{2+} (38). Propidium iodide staining experiments were done as described under "Experimental Procedures." Flow cytometry analysis showed that there were ~15% propidium iodide-permeable cells after treatment with Msp (30 μg/ml, 25 °C) for 40 min compared with ~9% for control cells (n = 5; $p < 0.05$). Therefore, most of the cells that were pretreated with Msp remained viable under the conditions of the experiments; those that were permeable to propidium iodide also exhibited less fura-2 staining and were not included in the measurements of $[Ca^{2+}]_i$. In contrast, after 24 h of exposure to Msp (10 μg/ml, 37 °C), there were ~66% propidium iodide-permeable cells after treatment (n = 5; $p < 0.05$), which is consistent with both the concentration and time course for the cytotoxicity of Msp complex reported previously (39). An alternative viability assay based on a replating and cell attachment method (40) showed no difference in viability

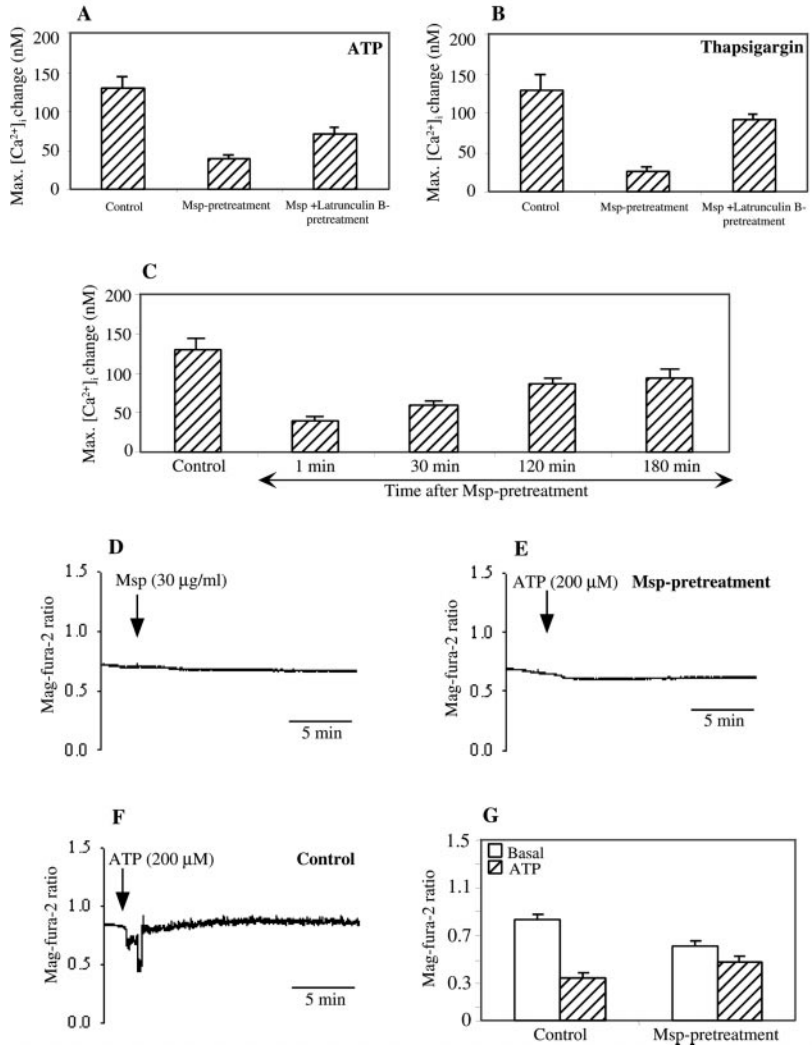

FIG. 3. **Msp inhibits ATP- and thapsigargin-induced Ca^{2+} release from internal stores.** Shown is the increase of $[Ca^{2+}]_i$ in single cells that were untreated (control) or pretreated with Msp (30 μg/ml, 25 °C, 40 min) or Msp and latrunculin B (1 μM, 25 °C, 40 min) and then incubated with 200 μM ATP (*A*) or 1 μM thapsigargin (*B*) in calcium-deficient EGTA-containing medium. The calcium-deficient media were switched immediately before experiments to reduce intracellular calcium depletion. The calcium-deficient media did not significantly reduce basal $[Ca^{2+}]_i$ over the time course of these experiments. Data are mean ± S.E. from $n = 8$ experiments showing maximum $[Ca^{2+}]_i$ change (in nM) induced by ATP or thapsigargin treatment. Pretreatment of cells with latrunculin B reverses the decrease in $[Ca^{2+}]_i$ change caused by Msp. *C*, summary of data (mean ± S.E.) from $n = 4-8$ experiments per group showing that the effects of Msp on ATP-induced Ca^{2+} transients were progressively reversed during increasing time periods following wash-out of free Msp from the assay buffer. *D–G*, Mag-fura-2 ratio data for estimation of $[Ca^{2+}]_{ER}$. Msp has no acute effect on base-line mag-fura-2 ratio (*D*). After the addition of ATP (200 μM), Msp pretreatment (30 μg/ml, 25 °C, 40 min) blocks ATP-induced reduction of mag-fura-2 ratio (*E*). In control cells with vehicle, the mag-fura-2 ratio is transiently reduced and then returns to base-line after refilling of ER stores (*F*). Summary data showing basal $[Ca^{2+}]_i$ and peak ATP-induced change of mag-fura-2 ratio (G; means ± S.E.; data are from $n = 9$ experiments). Note that pretreatment with Msp reduces the basal mag-fura-2 ratio by ~25%.

between control and Msp-challenged cells over a 60-min incubation (data not shown).

Msp Inhibits Ca^{2+} Release from Internal Stores—Outer membrane extracts of *T. denticola* inhibit agonist-induced increases of $[Ca^{2+}]_i$ in human gingival fibroblasts (17). We used two agonists capable of generating internal calcium release to study the effect of Msp pretreatment on calcium release from intracellular stores. ATP (200 μM) or thapsigargin (1 μM) was incubated with cells in calcium-free buffer containing 1 mM EGTA, a protocol that ensures that the induced calcium transients were attributable solely to release from internal calcium stores. Prior to the addition of agonists, the calcium-free buffer was quickly switched with the calcium-containing buffer to minimize calcium depletion from the cells. Indeed, measurement of the resting $[Ca^{2+}]_i$ values showed no significant reduction after EGTA treatment under these conditions ($[Ca^{2+}]_i$ ~150 nM). In cells treated with ATP, there was a nearly 2-fold increase of $[Ca^{2+}]_i$ above basal levels (Fig. 3*A*; $p < 0.05$). In contrast, pretreatment of cells with Msp (40 min; 25 °C) followed by stimulation with ATP showed a 70% reduction of the amplitude of ATP-induced calcium transients. In an identical experimental design, the mean amplitude of the calcium transient induced by thapsigargin was 80% less in the Msp-treated cells than controls (Fig. 3*B*; $p < 0.05$). We ran analogous experiments using 2-APB, an inhibitor thought to act by interference with $InsP_3$ receptors of the ER (9); 2-APB (75 μM) reduced the thapsigargin-releasable Ca^{2+} transients by ~50% (maximum $[Ca^{2+}]_i$ change (in nM) as follows: control cells, 127.5 ± 20.9; 2-APB-pretreated cells, 66.7 ± 6.7; $p < 0.05$; $n = 5$ per treatment). These experiments seemed to indicate that Msp interferes with the process of Ca^{2+} release from internal stores. The effect of Msp on ATP-induced Ca^{2+} transients was progressively reversed during increased time periods following wash-out of free Msp from the assay buffer (Fig. 3*C*). Notably, the cells were partially protected from the effect of Msp on both ATP- and thapsigargin-induced Ca^{2+} transients by pretreatment with the subcortical actin filament assembly inhibitor latrunculin B (1 μM; Fig. 3, *A* and *B*); the reversal was greater for the thapsigargin- than the ATP-challenged cells. Thus, the effect of Msp on the release of Ca^{2+} from ER stores in response to these agonists is probably functionally linked, in part, to its effects on the cytoskeleton and SOCs (see below).

For estimation of Ca^{2+} concentration in the ER stores, cells were loaded with mag-fura-2 according to the methods of Hofer *et al.* (30), and the mag-fura-2 emission ratio was calculated. Fluorescence microscopic examination of these cells showed that the dye was compartmentalized in discrete vesicular zones that closely resembled previously published images (30). Digitonin experiments as well as stimulation with ATP showed that the mag-fura-2 loading protocol was indeed reporting on calcium stores with properties similar to that of the endoplasmic reticulum. Msp produced no abrupt change in the mag-fura-2 ratio (Fig. 3*D*), but it did cause a slight decline in base-line measurements over the time course of the experiment. Pretreatment of cells with Msp (25 °C, 40 min) followed by incubation with ATP (200 μM) blocked the ATP-induced reduction of

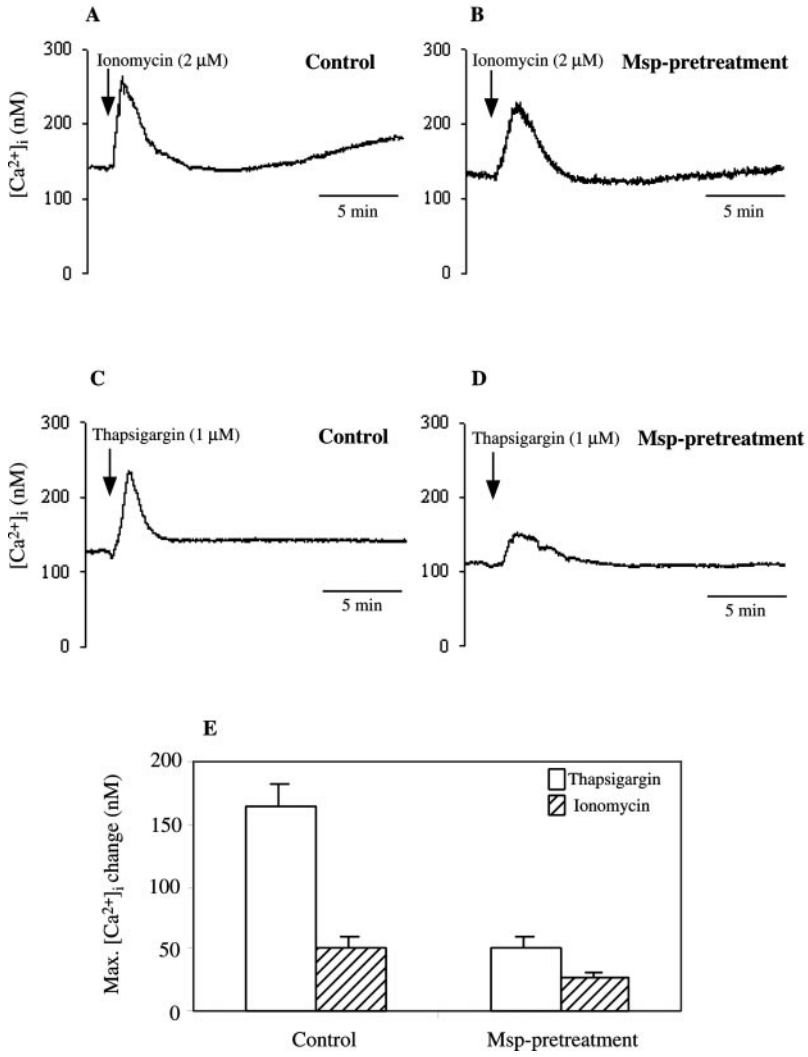

FIG. 4. **Msp alters ER store Ca^{2+} release kinetics.** Shown are representative calcium traces after the incubation of fura-2-loaded vehicle- or Msp-pretreated cells (30 μg/ml, 25 °C, 40 min) followed by the addition of ionomycin or thapsigargin. Typical calcium signals evoked by ionomycin (2 μM) are similar in vehicle-treated control cells (*A*) and Msp-pretreated cells (*B*). Shown are typical calcium signals evoked after thapsigargin (1 μM)-EGTA, showing different kinetics for $[Ca^{2+}]_i$ transients in control (*C*) and Msp-pretreated cells (*D*). The amplitude of the $[Ca^{2+}]_i$ transient is diminished, and the Ca^{2+} release is prolonged in the Msp-pretreated cells. *E*, summary data (mean ± S.E.) from $n = 4-8$ experiments per group showing that internal stores of both control and Msp-pretreated cells are comparably depleted of Ca^{2+} after thapsigargin (1 μM)-EGTA treatment, by measuring subsequent ionomycin (2 μM)-releasable Ca^{2+} transients.

the mag-fura-2 ratio (Fig. 3*E*). In contrast, treatment with ATP alone induced a sharp reduction of the mag-fura-2 ratio followed by a rapid recovery to base-line (Fig. 3*F*), indicating that ATP induced calcium efflux from ER stores. Traces of the mag-fura-2 ratio of single cells (Fig. 3, *E* and *F*) and summary analyses (Fig. 3*G*) showed that pretreatment with Msp lowered the basal mag-fura-2 ratio and the rate or amount of Ca^{2+} release from the ER stores upon ATP challenge. Collectively, these data seemed to suggest that Msp may either block calcium release or affect the kinetics of depletion and replenishment cycles of internal Ca^{2+} stores.

Alternatively, we considered that the combined effects of Msp and ER agonists may have so completely depleted intracellular stores that there was no more calcium to be released after ATP or thapsigargin treatment. Accordingly, we performed experiments in which cells were rapidly switched over to an EGTA (1 mM), calcium-free buffer prior to Msp or vehicle treatment and then treated with ionomycin (2 μM). In contrast to the ATP- or thapsigargin-induced response (Fig. 3, *A* and *B*; also see Fig. 4, *C* and *D*), the ionomycin-triggered Ca^{2+} transients were not different in control and Msp-pretreated cells. Indeed, both the amplitude (Fig. 4, *A* and *B*; summary analyses: vehicle = 263 ± 22 nM; Msp = 250 ± 25 nM; $p > 0.2$; $n = 4$ per treatment) and the kinetics of the transients were similar in vehicle- and Msp-pretreated fibroblasts. These results indicate that the inhibitory effect of Msp on the release of Ca^{2+} from the stores was not due to depletion of the stores prior to adding the agonists. Rather, Msp appears to specifically reduce the rate and/or the amount of agonist-induced Ca^{2+} release, *per se*. To determine whether Msp affected the total amount of the released Ca^{2+} or the kinetics of the release, we further analyzed the thapsigargin-induced $[Ca^{2+}]_i$ transients. To this end, the cells were incubated in the presence of EGTA (1 mM) and then challenged by thapsigargin. Finally, to assess the amount of releasable Ca^{2+} after thapsigargin treatment, ionomycin (2 mM) was added. The total Ca^{2+} released by thapsigargin, determined by measuring the area under the curve of $[Ca^{2+}]_i$ traces, was only marginally lower for the Msp-pretreated cells (vehicle = $9.13 \pm 0.25 \times 10^{-6}$ nM·s; Msp = $7.75 \pm 0.19 \times 10^{-6}$ nM·s; $p < 0.005$). Yet, Msp pretreatment clearly reduced the amplitude of the Ca^{2+} transient and slowed down the rate of Ca^{2+} release and return of the transient to base-line values (Fig. 4, *C* and *D*). Moreover, the thapsigargin-sensitive Ca^{2+} stores of the Msp-pretreated and control cells were comparably depleted, as shown by the similar residual Ca^{2+} release upon the addition of ionomycin (Fig. 4*E*). Taken together, this series of experiments indicates that Msp interferes with the process of Ca^{2+} release from ER stores, seen as the lower amplitude and altered kinetics of $[Ca^{2+}]_i$ transients, despite its minimal effect on the amount of Ca^{2+} released over time.

Msp Inhibits Store-operated Calcium Influx—We determined if Msp may inhibit the refilling of internal Ca^{2+} stores by blocking the influx of extracellular calcium following depletion of these stores. Cells were pretreated with thapsigargin, and the medium was augmented with EGTA (1 mM) to deplete the stores and prevent refilling. As shown above, after sufficient

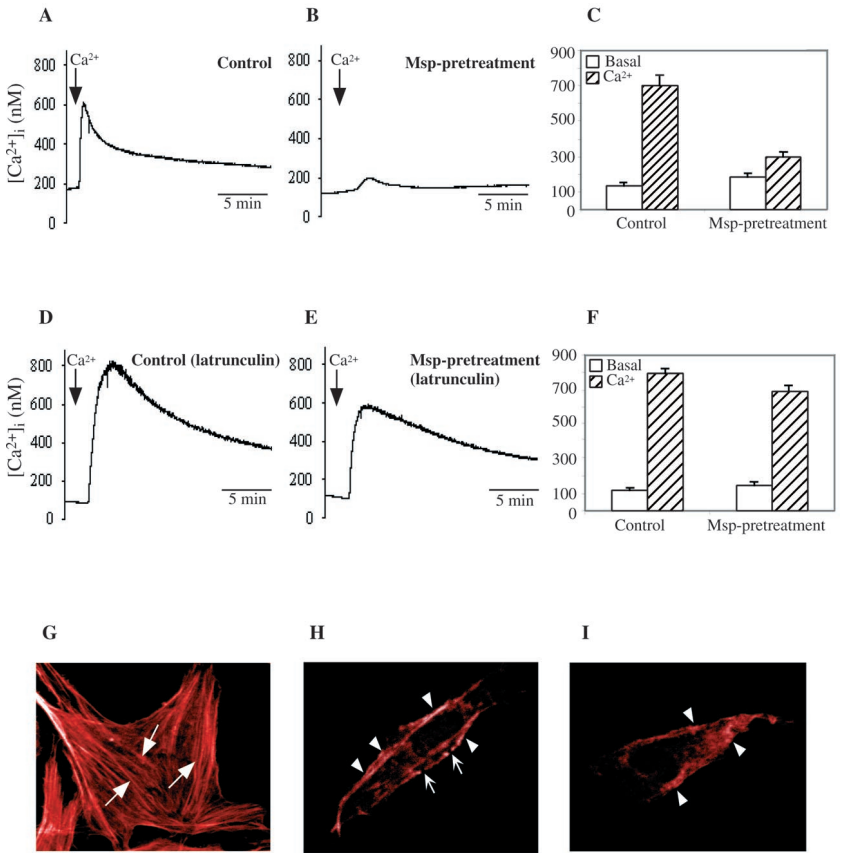

FIG. 5. **Msp inhibits store-operated Ca^{2+} influx in fibroblasts.** Shown are representative calcium traces after the incubation of fura-2-loaded cells with 1 μM thapsigargin in calcium-deficient medium for 30 min, followed by the addition of 2 mM extracellular calcium. Shown are typical calcium signals evoked by the addition of 2 mM extracellular calcium in vehicle-pretreated control cells (*A*) and Msp-pretreated cells (30 μg/ml, 25 °C, 40 min) (*B*). *C*, summary data from $n = 9$ experiments showing basal $[Ca^{2+}]_i$ and peak $[Ca^{2+}]_i$ after the addition of extracellular calcium (means ± S.E. of $[Ca^{2+}]_i$ in nM above base line). *D* and *E*, typical calcium signals for latrunculin B-pretreated cells with and without Msp challenge. Cells were pretreated with 1 μM latrunculin followed by the protocols described in Fig. 5, *A* and *B*, respectively. *F*, summary data from $n = 5$ experiments comparing Msp-challenged and control cells that had been pretreated with latrunculin B ($n = 5$ independent experiments; means ± S.E. of $[Ca^{2+}]_i$ in nM). *G–I*, confocal microscopy of human gingival fibroblasts stained with rhodamine-phalloidin showing assembly of subcortical actin induced by Msp. *G*, vehicle-treated control cells. *H*, fibroblasts pretreated with Msp for 5 min. Note that rhodamine phalloidin staining for actin filaments in stress fibers is prominent in control cells (*G*; *arrows*) but is lost in Msp-treated cells, while staining near the cortex is greatly intensified (*arrowheads*; *H*). The increased density of actin filaments in subcortical regions was confirmed by quantitative fluorescence spectrophotometry (see "Results"). Pretreatment of cells with Msp for 45 min induces almost complete depolymerization of stress fibers and the formation of a dense subcortical actin filament network (*I*).

time, the ER stores were similarly depleted in control and Msp-pretreated cells. After the addition of $CaCl_2$ (2 mM), $[Ca^{2+}]_i$ rose to a peak and then returned to a somewhat higher base-line (Fig. 5*A*). The maximum influx of Ca^{2+} was diminished >2-fold ($p < 0.05$) in Msp-treated cells (Fig. 5, *B* and *C*). This finding suggests that Msp may have inhibited the influx of extracellular calcium through SOCs and uncoupled the feedback connection between internal Ca^{2+} release and store-operated calcium entry.

Msp Induces Actin Reorganization in Human Gingival Fibroblasts—Since *T. denticola* causes actin rearrangement in fibroblasts (11), we determined if Msp may inhibit activation of SOCs by promoting actin assembly (5, 7). Cells were pretreated with latrunculin B (1 μM) to prevent subcortical actin assembly and incubated with vehicle or Msp, and then intracellular calcium was depleted with thapsigargin and EGTA as described for cells in Fig. 5*A*. Under these conditions, internal Ca^{2+} stores of Msp-pretreated and control cells were comparably depleted. The amplitude of acute Ca^{2+} transients in response to Msp (30 μg/ml) was unaffected by latrunculin B (maximum $[Ca^{2+}]_i$ change (in nM): control cells, 258.8 ± 50.0; latrunculin B-pretreated cells, 221.7 ± 15.9; $n = 4$ per treatment). Yet, under the same conditions, Msp barely inhibited Ca^{2+} depletion-induced Ca^{2+} influx (Fig. 5, *D–F*) when compared with its strong inhibition in cells that were not treated with latrunculin B (Fig. 5*C*). Since these data indicated that the mechanism by which Msp uncouples SOCs is related to its effects on actin assembly, we used confocal microscopy to examine the effects of Msp on the distribution of actin filaments (Fig. 5, *G–I*). After a 5-min treatment with Msp (30 μg/ml), there was an almost complete loss of rhodamine-phalloidin-stained actin filaments in stress fibers and a greatly increased staining in the subcortical region. After treatment of cells with Msp for 45 min, the increased density of actin filaments subjacent to the plasma membrane was maintained. These data suggested that the early Msp-induced calcium transients may have promoted the assembly of subcortical actin filaments, which in turn uncoupled the SOCs from the intracellular stores. Accordingly, we examined if chelation of the Msp-induced calcium transient would prevent the formation of subcortical actin filaments. Cells were preincubated (or not) with 1,2-bis(2-aminophenoxy)ethane-*N*,*N*,*N*′,*N*′-tetraacetic acid acetoxymethyl ester (3 μM) for 15 min prior to Msp or vehicle treatment for 30 min. Fixed cells were stained with rhodamine phalloidin, and subcortical actin filaments were measured by quantitative fluorescence photometry. Consistent with the images obtained by confocal microscopy, Msp induced substantial increases of actin filament staining in subcortical zones (vehi-

cle = 52 ± 8 fluorescence units; Msp = 129 ± 24 fluorescence units; $p < 0.02$; $n = 10$ cells/treatment). In contrast, preincubation with 1,2-bis(2-aminophenoxy)ethane-*N*,*N*,*N*′,*N*′-tetraacetic acid acetoxymethyl ester abrogated the Msp-induced actin assembly (vehicle = 40 ± 5 fluorescence units; Msp = 47 ± 5 fluorescence units; $p > 0.2$; $n = 10$ cells/treatment).

DISCUSSION

The central finding in this investigation is that the major surface protein of the spirochete *T. denticola* promotes subcortical actin assembly that subsequently perturbs calcium signaling in human fibroblasts. Since calcium signals are tightly and reciprocally linked to regulation of the actin cytoskeleton (2), microbial perturbation of this system has profound effects on cell regulation. Not only is the activity of actin-binding and -severing proteins determined by local concentrations of calcium, but the assembly of subcortical actin filaments evidently affects the coupling of two key components of store-operated calcium flux: depletion/refill cycles of ER store Ca^{2+} and Ca^{2+} entry through SOCs (5–7). Since store-operated flux is a major pathway by which intracellular Ca^{2+} concentration is regulated in response to extracellular agonists, it occurred to us that pathogenic microoganisms may perturb host cells by affecting their store-operated calcium pathways. In contrast to the exotoxins or surface proteins of bacteria that stimulate host cell calcium signaling, our previous data have shown that protein(s) in the *T. denticola* outer membrane inhibit calcium signals in gingival fibroblasts (17). In this study, we examined the mechanism by which the major outer sheath protein of *T. denticola*, Msp, perturbs calcium signaling. We have identified two potentially pathological responses: (i) an early, acute rise in $[Ca^{2+}]_i$ due to increased conductance across the plasma membrane and (ii) a delayed perturbation of store-operated calcium flux. The latter includes two unprecedented effects, alteration of ER Ca^{2+} release kinetics and inhibition of Ca^{2+} entry through putative SOCs. We have also provided substantial support for the hypothesis that Ca^{2+} ER stores and SOCs are conformationally coupled (5–7) by using the gingival fibroblast as a target cell and Msp as a biologically relevant antagonist isolated from a pathogenic bacterium.

Msp bound and clustered into complexes on the cell surface, perhaps due to receptor aggregation after ligand occupancy. Both the bacterium *T. denticola* and Msp can bind to extracellular matrix proteins (37, 41), which could provide the initial adhesion of Msp to gingival fibroblasts. Indeed, abundant cell surface-associated fibronectin (23) could have bound Msp and effectively lowered its bioavailability for the induction of Ca^{2+} transients in our experiments. Nevertheless, when sufficient amounts of Msp were added (~160 nM), there was a robust intracellular Ca^{2+} response.

Msp failed to induce Ca^{2+} transients in cells incubated in Ca^{2+}-free buffer and failed to stimulate Ca^{2+} release from ER stores. As Msp increased manganese conductance, it is evident that the Msp-induced calcium transients probably arose from the influx of external Ca^{2+}. Indeed, we found that the elapsed time following exposure of the cells to Msp and both the ensuing peak in cytoplasmic Ca^{2+} and the rapid quenching of fluorescence by Mn^{2+} was coincidentally ~90 s. Acute Ca^{2+} influx may be due to activation of ligand-gated channels (42) or from the translocation of some of the bound Msp into the plasma membrane to increase plasma membrane conductance to cations. This latter notion is consistent with earlier evidence showing that Msp can form transient, ion-permeable channels in HeLa cells (22, 39) and is reminiscent of recent reports on the formation of cation-permeable channels by complexes of α-latrotoxin oligomers (43). However, our flow cytometry measurements with a bisoxonol dye showed no significant loss of membrane potential, indicating that there was no general increase of cation conductance (*e.g.* sodium). Thus, it appears that Msp represents a novel type of bacterial cytotoxin whose immediate pathogenic effect is the specific promotion of increased calcium conductance.

Longer term experiments (~30 min) showed that Msp reduced ATP- and thapsigargin- induced $[Ca^{2+}]_i$ transients and blocked subsequent Ca^{2+} entry following thapsigargin treatment, indicating that Msp uncouples physiologic store-operated calcium flux. These findings were not due to prior store depletion, since ionomycin induced immediate and equivalent calcium release in control and Msp-pretreated cells in calcium-free buffer. Further experiments with ionomycin showed that thapsigargin-sensitive Ca^{2+} stores were comparably depleted in control and Msp-pretreated cells. Yet, the amplitude of thapsigargin-induced calcium transients was clearly decreased, and the kinetics of Ca^{2+} release were clearly altered in the Msp-pretreated cells. The mechanisms accounting for this unprecedented effect of a bacterial toxin are not entirely clear. They may involve perturbation of Ca^{2+} release and/or reuptake into ER or other internal Ca^{2+} stores and may be affected by *de novo* actin filament assembly near the ER and other calcium-containing organelles. Notably, the reduction of thapsigargin- and ATP- induced Ca^{2+} transients by Msp was reversed in latrunculin B-pretreated cells. Thus, the altered kinetics of Ca^{2+} release and/or replenishment of ER stores following incubation of Msp-pretreated cells with agonists may be caused, in part, by actin filament reorganization. Evidently, the key element in the perturbation of store-operated calcium flux by Msp is that it induces a calcium-dependent assembly of subcortical actin filaments in gingival fibroblasts, suggesting that Msp may uncouple the ER and Ca^{2+} channels in the plasma membrane.

There is growing experimental support for conformational coupling as a principal regulatory mechanism that links Ca^{2+} store depletion and Ca^{2+} influx through SOCs (1). Experimental strategies using drugs that affect actin assembly, translocation of actin to the cell periphery, and the association of actin and actin-binding proteins with the plasma membrane support the hypothesis that *de novo* assembly of an actin filament network subjacent to the plasma membrane impairs conformational coupling (5, 7). We have shown previously that *T. denticola* induces rearrangement of actin (11, 12, 15), with a proportional shift in actin filaments from the stress fiber-rich ventral interface to the dorsal area of the cell (14). Here, we observed that the Msp-induced calcium transient is required for subcortical actin filament assembly, and this actin network is formed contemporaneously with the block of store-operated calcium flux. However, in cells pretreated with latrunculin B to inhibit actin filament assembly, both Ca^{2+} release from thapsigargin-sensitive stores and Ca^{2+} entry following Ca^{2+} store depletion were hardly affected upon challenge with Msp. We interpret these findings to indicate that the Msp of *T. denticola* perturbs store-operated calcium flux by uncoupling SOCs, and we provide corroborating evidence for actin assembly-dependent conformational coupling of SOCs in an additional cell type, the human gingival fibroblast.

The binding of many pathogenic bacterial species or their toxins to host cells can elicit intracellular calcium signals that are often associated with substantial cytoskeletal rearrangement (44–48). Some bacterial outer membrane porins can even translocate to the plasma membrane of target cells and induce apoptosis secondary to the rapid influx of Ca^{2+} (49, 50). For another example, cholera toxin increases Ca^{2+} current through calcium release-activated calcium channels in mast cells (11). Therefore, pathogens may induce cytotoxicity by causing ab-

normally elevated cytoplasmic Ca^{2+} levels in target cells, which is one of the acute effects of *T. denticola* outer membrane proteins (17), specifically Msp. Although presently unique, our central finding is that the major surface protein of the spirochete *T. denticola* inhibits calcium flux by uncoupling store-operated calcium channels. Conceivably, this may well become a more general theme of pathogenic host-parasite interactions. Indeed, our data suggest a general mechanism by which pathogens can block one of the key cellular signaling pathways for responses to natural agonists such as growth factors, extracellular matrix proteins, cytokines, and a variety of other mediators of intercellular communication networks. Pharmacological intervention to block this pathway of bacterial pathogenicity may provide a novel approach to inhibit the cytotoxic effects of some species of spirochetes and other pathogens that cause chronic disease.

Acknowledgments—We thank David A. Grove, Pam Arora, and Wilson Lee for technical assistance. We thank Pauline Hannam and Barry C. McBride for supplying the anti-Msp polyclonal antibodies and for helpful advice about the isolation of enriched Msp. We thank Milton Charlton and Philip Sherman for insightful criticism of the draft manuscript.

REFERENCES

1. Berridge, M. J., Lipp, P., and Bootman, M. D. (2000) *Science* **287,** 1604–1605
2. Janmey, P. A. (1994) *Annu. Rev. Physiol.* **56,** 169–191
3. Putney, J. W., and Bird, G. S. (1993) *Cell* **75,** 199–201
4. Parekh, A. B., and Penner, R. (1997) *Physiol. Rev.* **77,** 901–930
5. Kourie, J. I., and Shorthouse, A. A. (2000) *Am. J. Physiol.* **278,** C1063–C1087
6. Suchyna, T. M., Johnson, J. H., Hamer, K., Leykam, J. F., Gage, D. A., Clemo, H. F., Baumgarten, C. M., and Sachs, F. (2000) *J. Gen. Physiol.* **111,** 583–598
7. McCloskey, M. A., and Zhang, L. (2000) *J. Cell Biol.* **148,** 137–146
8. Patterson, R. L., van Rossum, D. B., and Gill, D. L. (1999) *Cell* **98,** 487–499
9. Ma, H.-T., Patterson, R. L., van Rossum, D. B., Birnbaumer, L., Mikoshiba, K., and Gill, D. L. (2000) *Science* **287,** 1647–1651
10. Rosado, J. A., Jenner, S., and Sage, S. O. (2000) *J. Biol. Chem.* **275,** 7527–7533
11. Baehni, P., Song, M., McCulloch, C. A. G., and Ellen, R. P. (1992) *Infect. Immun.* **60,** 3360–3368
12. De Filippo, A. B., Ellen, R. P., and McCulloch, C. A. (1995) *Arch. Oral. Biol.* **40,** 199–207
13. Uitto, V.-J., Pan, Y. M., Leung, W. K., Larjava, H., Ellen, R. P., Finlay, B. B., and McBride, B. C. (1995) *Infect. Immun.* **63,** 3401–3410
14. Yang, P. F., Song, M., Grove, D. A., Ellen, R. P. (1998) *Infect. Immun.* **66,** 696–702
15. Battikhi, T., Lee, W., McCulloch, C. A. G., and Ellen, R. P. (1999) *Infect. Immun.* **67,** 1220–1226
16. Ellen, R. P. (1999) *Micr. Infect.* **1,** 621–632
17. Ko, K. S., Glogauer, M., McCulloch, C. A., Ellen, R. P. (1998) *Infect. Immun.* **66,** 703–709
18. Rosado, J. A., and Sage, S. O. (2000) *J. Biol. Chem.* **275,** 9110–9113
19. Rosado, J. A., and Sage, S. O. (2000) *Biochem. J.* **347,** 183–192
20. Rosado, J. A., and Sage, S. O. (2000) *Biochem. J.* **350,** 631–635
21. Egli, C., Leung, W. K., Müller, K.-H., Hancock, R. E. W., McBride, B. C. (1993) *Infect. Immun.* **61,** 1694–1699
22. Mathers, D. A., Leung, W. K., Fenno, J. C., Hong, Y., McBride, B. C. (1996) *Infect. Immun.* **64,** 2904–2910
23. Ellen, R. P., Song, M., McCulloch, C. A. G. (1994) *Infect. Immun.* **62,** 3033–3037
24. Laemmli, U. K. (1970) *Nature* **277,** 680–685
25. Ellen, R. P., Ko, K. S.-C., Lo, C.-M., Grove, D. A., and Ishihara, K. (2000) *J. Mol. Microbiol. Biotechnol.* **2,** 581–586
26. Scopes, R. K., and Smith, J. A. (1997) *Current Protocols in Molecular Biology*, Vol. 2 (Ausubel, F. N., Brent, R., Kingston, R. E., Moore, D. D., Seidman, J. G., Smith, J. A., and Struhl, K., ed) pp. 10.8.1–10.8.17, John Wiley & Sons, Inc., New York
27. Fenno, J. Müller, K.-H., McBride, B. C. (1996) *J. Bacteriol.* **178,** 2489–2496
28. Pender, N., and McCulloch, C. A. G. (1991) *J. Cell Sci.* **100,** 187–193
29. Etter, E. F., Kuhn, M. A., Fay, F. S. (1994) *J. Biol. Chem.* **269,** 10141–10149
30. Hofer, A. M., Landofi, B., Debellis, L., Pozzam, T., and Curci, S. (1998) *EMBO J.* **17,** 1986–1995
31. Golovina, V. A., and Blaustein, M. P. (1997) *Science* **275,** 1643–1648
32. Grynkiewicz, G., Poenie, M., and Tsien, R. Y. (1985) *J. Biol. Chem.* **260,** 3440–3450
33. Bibby, K. J., and McCulloch, C. A. G. (1994) *Am. J. Physiol.* **266,** C1639–C1649
34. Seidl, J., Knuechel, R., Kunz-Schughart, L. A. (1999) *Cytometry* **36,** 102–111
35. Arora, P. D., Manolson, M., Downey, G. P., and McCulloch, C. A. G. (2000) *J. Biol. Chem.* **275,** 35432–35441
36. Lee, W., Sodek, J., and McCulloch, C. A. (1996) *J. Cell. Physiol.* **168,** 695–704
37. Haapasalo, M., Müller, K.-H., Uitto, V.-J. Leung, W. K., McBride, B. C. (1992) *Infect. Immun.* **60,** 2058–2065
38. Nicotera, P., and Orrenius, S. (1998) *Cell Calcium* **23,** 173–180
39. Fenno, J. C., Hannam, P. M., Leung, W. K., Tamura, M., Uitto, V.-J., and McBride, B. C. (1998) *Infect. Immun.* **66,** 1869–1877
40. Kulkarni, G. V., and McCulloch, C. A. G. (1994) *J. Cell Sci.* **107,** 1169–1179
41. Dawson. J. R., and Ellen, P. R. (1990) *Infect. Immun.* **58,** 3924–3928
42. Schwartz, M. A. (1993) *J. Cell Biol.* **120,** 1003–1010
43. Orlova E. V., Rahman, M. A., Gowen, B., Volynski, K. E., Ashton, A. C., Manser, C., van Heel, M., and Ushkaryov, Y. A. (2000) *Nat. Struct. Biol.* **7,** 48–53
44. Baldwin, T. J., Ward, W., Aitken, A., Knutton, S., and Williams, P. H. (1991) *Infect. Immun.* **59,** 1599–1604
45. Pace J, Hayman, M. J., and Galan, J. E. (1993) *Cell* **72,** 505–514
46. Dytoc, M., Fedorko, L., and Sherman, P. M. (1994) *Gastroenterology* **106,** 1150–1161
47. Källström, H., Islam, S., Berggren, P.-O., and Jonsson, A.-B. (1998) *J. Biol. Chem.* **273,** 21777–21782
48. Izutsu, K. T., Belton, C. M., Chan, A., Fatherazi, S., Kanter, J. P., Park, Y., and Lamont, R. J. (1996) *FEMS Microbiol. Lett.* **144,** 145–150
49. Buommino, E., Morcelli, F., Metafora, S.,, Rossano, F., Perfetto, B., Baroni, A., and Tufano, M. A. (1999) *Infect. Immun.* **67,** 4794–4800
50. Muller, A., Gunther, D., Dux, F., Naumann, M., Meyer, T. F., and Rudel, T. (1999) *EMBO J.* **18,** 339–352
51. Fenno, J. C., Wong, G. W. K., Hannam, P. M., Müller, K.-H., Leung, W. K., and McBride, B. C. (1997) *J. Bacteriol.* **179,** 1082–1089